Statistical iterative reconstruction for streak artefact reduction when using multidetector CT to image the dento-alveolar structures

doi: http://dx.doi.org/10.1259/dmfr.20130373

(a) Title:

Statistical iterative reconstruction for streak artefact reduction when using multi-detector CT to image the dento-alveolar structures

(b) Category of paper:

Research Article

(c) Authors:

1. Jian Dong *MEng* [1] (Affiliation 1)
2. Yoshihiko Hayakawa *PhD* [1] (Affiliation 1)
3. Cornelia Kober *PhD* [2] (Affiliation 2)

(d) Affiliations:

1. Dept. of Computer Science, Faculty of Engineering, Kitami Institute of Technology
   165 Koencho, Kitami, Hokkaido 090-8507 JAPAN
2. Faculty of Life Sciences, Hamburg University of Applied Sciences
   Lohbruegger Kirchstr. 65, Hamburg D-21033 GERMANY

(e) A shortened version of the title

Statistical iterative reconstruction for CT artefact reduction

(f) Grants

1. Japan-Germany Joint Research Project, Bilateral Program of the Japan Society of the Promotion of Science (JSPS), 2010-2011
2. Grants-in-Aid for Scientific Research, Ministry of Education, Culture, Sports, Science and Technology (MEXT) of Japan, 2012-2013

(g) Corresponding Author:

Mr. Jian Dong, MEng.

Email(1): d[redacted].co.jp Email(2): d[redacted].kitami-it.ac.jp

Phone:+81-157-26-[redacted] FAX: +81-157-26-[redacted]

Postal Address: Dept. of Computer Science, Faculty of Engineering,
Kitami Institute of Technology
165 Koencho, Kitami, Hokkaido 090-8507 JAPAN

(a) Title:

Statistical iterative reconstruction for streak artefact reduction when using multi-detector CT to image the dento-alveolar structures

Abstract

***Objectives*:** When metallic prosthetic appliances and dental fillings exist in the oral cavity, the appearance of metal-induced streak artefacts are not avoidable in CT images. The study was to develop a method for artefact reduction using the statistical reconstruction on MD (multi-detectors row) CT images.

***Methods*:** Adjacent CT images often depict similar anatomical structures. Therefore, reconstructed images with weak artefacts were attempted using projection data of an artefact-free image in a neighboring thin slice. Images with moderate and strong artefacts were continuously processed in sequence by successive iterative restoration where projection data was generated from the adjacent reconstructed slice. First, the basic maximum likelihood-expectation maximization (ML-EM) algorithm was applied. Next, the ordered subset-expectation maximization (OS-EM) algorithm was examined. Alternatively, a small region of interest (ROI) setting was designated. Finally, the GPGPU (general purpose graphic processing unit) machine was applied in both situations.

***Results*:** The algorithms reduced metal-induced streak artefacts on MDCT images when the sequential processing method was applied. The OS-EM and small ROI reduced the processing duration without apparent detriments. GPGPU realized the high performance.

***Conclusions*:** A statistical reconstruction method was applied for the streak artefact reduction. The alternatives of algorithms applied were effective. Both software and hardware tools, such

as OS-EM, small ROI and GPGPU achieved fast artefact correction.

Keywords: CT, X-ray; statistical iterative reconstruction; streak artefact reduction; dento-alveolar region

Introduction

Statistical reconstruction has been developed for noise reduction on images and radiation exposure reduction to patients.[1-8]

When CT examinations are carried out to image the dental-alveolar region and there are metallic prosthetic appliances and restoration dental materials in the oral cavity, the appearance of metal-induced streak artefacts is not avoidable.[9-14] Fixed metallic prosthetic appliances are usually made from high atomic-number, high-density materials. Similar artefacts are also observed by the presence of other metallic biomaterials.[15-21] The streak artefacts caused by metallic materials on multi-detector row CT (MDCT) images are intense and radial.

Metallic biomaterials that are not only in the oral and maxillofacial region but also in other body regions cause loss of portions of the projection data due to extremely high x-ray absorption coefficients.[12,13,19,21] Resulting sinogram patterns show the image corruption from such missing data. The traditional CT reconstruction method, the filtered back-projection (FBP) algorithm, cannot deal with such metal-induced inconsistencies. Hence, several alternative algorithms have been proposed for metal-induced streak artefact reduction.[12,13,15-19,21] These repair the partly corrupted sinogram data by either the replacement by intact data or by interpolation.

Statistical reconstruction algorithms are an old idea for image construction; however, they

can be considered relatively new technology when applied to quality improvement of CT images.[1,2,4-6,8,9,21-24] In previous studies, statistical reconstruction algorithms have been applied not only for image-quality improvement, but also for streak artefact reduction.[22-24] The present investigation focused on the fact that there were artefact-free slices next to slices with heavy streak artefacts, and that such slices depicted morphologically almost identical portions of anatomical structures. The maximum likelihood-expectation maximization (ML-EM) reconstruction algorithm was attempted with successive iterative restoration to reduce metal-induced streak artefacts.[22,23]

Previously, Kondo, *et al*. used the ML-EM algorithm to process a MDCT slice with heavy artefacts by using the projection data of the artefact-free slice on the neighboring slice.[22] There were 7 slices (0.5 mm for a single slice) between the slice being processed and the artefact-free slice. Dong, *et al*. applied the successive iterative restoration method.[23]

Statistical reconstruction algorithms usually necessitate a huge amount of computational effort, and are sometimes termed the algebraic reconstruction technique. The ML-EM algorithm, which was used in previous studies, was a very time-consuming procedure.[22,23] It took more than 6 minutes to reconstruct a 512 x 512 matrix image for 50-cycle iterations using a desktop PC.[23] Subsequently, Dong, *et al*. applied the ordered subset-expectation maximization (OS-EM) algorithm as a solution to speeding computation.[24] Further performance improvement was achieved by using a small ROI (region of interest) setting

combined with successive and reverse processing methods.[24]

The purpose of the presently reported study was to investigate use of a very small ROI setting, and fast calculation by the CUDA (compute unified device architecture) programming optimized for the GPGPU (general purpose graphic processing unit).

Materials and methods

Image acquisition

In this report MDCT image volumes used for the clinical diagnosis of the jaw-deformity were processed. The subject was a 32-years-old female at the time of pre-surgical imaging, and had been subsequently re-imaged following surgery. IRB approval was forthcoming. The subject consented to the use of her CT images for the study. The image volumes were acquired using a LightSpeed VCT (GE Healthcare, USA). The exposure parameters were: 120 kV, 361 mAs, and slice thickness was 1.3 mm. The pixel matrix of each slice was 512 x 512. Severe metal-induced streak artefacts occurred due to several metallic tooth crowns in the maxilla and mandible and orthodontic appliances.

Projection data acquisition

Projection data acquisition was carried out as described in previous reports.[22-24] Each pixel of the image has a CT number, which is proportional to x-ray transparency. When the x-ray traverses each pixel, the shape of each pixel is usually a trapezoid, depending on the angle

between the projection and each pixel square. In special cases, projection shapes of square pixels become either a square at 0°, 90°, 180°, and 270° or a triangle at 45°, 135°, 225°, and 315° when the coordinate axes are set along edges of the image (Figure 1). The image matrix contained 512 pixels. During the detectability calculation, the value is accumulated by adding the respective pixels' CT number. If the shape of the projection is not square, the detectability will be divided by the center of the detector element and neighboring elements. The projection data were acquired in 360 directions with 1 degree intervals, so the pixel number was 512 x 360.

Successive iterative restoration

Generally, CT examinations with thin slice thicknesses are carried out in the dento-alveolar region, and adjacent CT slices often depict very similar anatomical structures. The current trial was to reconstruct the CT image containing streak artefacts using the projection data of the adjacent image.[22-24]

In previous studies, we compared two different processing methods.[23,24] First, we obtained the projection data of the artefact-free image. Continuous neighboring images were processed using the same intact image's projection data.[23] Alternatively, while the projection data acquisition of the artefact-free image was carried out similarly, projection data to reduce the artefact used only immediately adjacent slice. After the slice was reconstructed, the projection data of the processed image was obtained, and then applied to process the

neighboring slice. As so on, using the 'successive' iterative restoration method for processing all images.[24] For the present report, the successive method was employed.

Iterative restoration: ML-EM and OS-EM methods

As the iterative restoration method, we used two algorithms; namely, ML-EM and OS-EM. The ML-EM algorithm results in an approximation between the processing image and the target image. The formulation of ML-EM algorithm is described as follows:

$$\lambda_j^{(k+1)} = \frac{\lambda_j^{(k)}}{\sum_{i=1}^{n} C_{ij}} \sum_{i=1}^{n} \frac{y_i C_{ij}}{\sum_{j'=1}^{m} C_{ij'} \lambda_{j'}^{(k)}}$$

Where λ (Lambda) is the output value of each pixel; *k*, the counter of iteration (loop variable); *j*, the number of pixels (1- m), m = 262,144 if the image matrix is 512 x 512; *i*, the number of detector's element (1 - n); *Cij*, detecting probability as the relation of pixel (*i*) and detector's element (*j*); and *yi*, the projection data by the pixel (*i*).

We applied the ML-EM algorithm to reconstruct images following the steps shown in Table 1. An artefact-free image is needed to process a CT image having streak artefacts (Step 1). Based on the projection data acquisition rules, the projection data of two images can be calculated (Step 2). Then the two projection data sets are compared pixel by pixel. When the values are different, the pixel value which belongs to projection data of artefact-containing image is modified due to another value. The new value must be calculated using the value of artefact-free image's projection data as a reference (Step 3). After every pixel is compared on the projection data, a new projection data are produced. Next, the back projection operation is

executed based on the newly produced projection data (Step 4). Then a new image, which contains both features of the artefact-free (or artefact-reduced) and artefact-containing images, can be obtained (Step 5). More iterative operations will lead to the new image appearing features of the artefact-free image dominantly (Step 6). Of steps, the key procedure is the process of comparing the projection data of intact and the newest one, and then making an approximation between them.

The OS-EM algorithm was also used as the successive iterative reconstruction algorithm in this work as same as a previous work.[24] The OS-EM algorithm, which is based on the ML-EM algorithm, divides the projection data to several subsets and carries out the projection, comparison, back projection, and renewal to only the data belonging to the given subset. Suppose that there are 24 projection angles in calculating projection data. The 24 projection angles can be divided into {1, 2, 3, 4, or 6} subsets. For the OS-EM algorithm, the image quality factor, namely the image update number, is the product of subset numbers and iteration times (image update number = subset number x iteration times). Therefore, there will be more image updates during one time iteration and as a result images can be reconstructed quickly. In our previous report, combinations of subset number (either 4 or 8) and iteration numbers (either 5 or 10) were examined, and as a result, the optimal combination of subset number and iteration times was derived to be subset = 8 and iteration = 10, and streak artefacts could be reduced at utmost on this condition.[24] Then, we chose this combination

decisively in this study.

The processing was executed based on the C-language program. The performance of the computer we used was as follows: an Intel Core 2 Duo central processing unit, running at 3.16 and 2.83 GHz, and a Windows Vista operating system.

ROI (Region of Interest) setting

Because streak artefacts appeared only surrounding the teeth, we did the segmentation to CT slices only for the region of the teeth. A simple rectangular ROI was used for the segmentation each time. The projection data were calculated only from the tooth area; therefore, the density of the center part became brighter in the projection data image (sinogram), and the soft tissue components seemingly disappeared at the image periphery.

CUDA programming for GPGPU Machine

A high performance GPGPU machine was used to execute the streak artefact reduction algorithm. Three CUDA-supporting GPU, NVIDIA GeForce GTX 680, were installed. The programming language used was CUDA, which is a specific C-language programming being necessary for the powerful operation of GPGPU machines. A kernel function in the device code can divide a process to synchronous multi threads. According to the steps of successive iterative OS-EM algorithms, the procedure of calculating projection data was repetitively executed for iteration times. The projection data calculating procedure was divided into synchronous multi threads according to projection acquisition angles.

Results

Images shown from Figure 2 to Figure 7 are from a jaw deformity (mandibular retraction) case. Images shown in Figure 2 are original images. They were acquired as the preoperative evaluation of bone morphology in mandible for the jaw deformity treatment. No orthodontic devices or titanium plates were present. Figure 3 is an artefact-free image which is the adjacent image to the far left one on the top row in Figure 2. Its projection data (sinogram) is illustrated on the right. As indicated in the methodology, the OS-EM successive iterative restoration algorithm was applied on images. Resultant images are shown in Figure 4 and they are corresponding to the order shown in Figure 2. On the original images in Figure 2, streak artefacts occurred from several tooth crown metallic restorations. Processing substantially reduced streak artefacts (Figure 4).

After receiving 3-years of orthodontic treatment, the patient had a surgical operation, using a sagittal split ramus osteotomy (SSRO). The CT images shown in Figure 5 were scanned for the post-operative diagnosis. Orthodontic wire and brackets, bone screws or titanium plates can be observed on some specific CT slices. The image in Figure 6 is an artefact-free image, which is attached with the projection data (sinogram), and it is the adjacent image of the far left one on the top row of Figure 5. As explained in the methodology, the OS-EM successive iterative restoration algorithm was applied. The resultant images are shown in Figure 7 and

they are corresponding to the order shown in Figure 5. The original images in Figure 5, show streak artefacts which were intense. The artifacts were caused not only by dental restorative materials but also by orthodontic wire, brackets and titanium plates. On the resultant images in Figure 7, streak artefacts caused by every kind of metallic materials were reduced effectively. Tooth shape reverted to the original states on the former images, while some false anatomical structure occurred on incisor and cuspid areas on the latter images.

In addition, we reconstructed 3D images using images from Figure 5 and Figure 7. The OsiriX, three-dimensional medical & photographic DICOM viewer, was used. The resulting 3D images are shown in Figure 8 and they represented only a thin part of maxilla. The left and middle images in Figure 8 were merged respectively from slices where streak artefacts appeared (Figure 5) and were reduced (Figure 7). The image on the right of Figure 8 presented a simultaneous visualization of the left and middle images with different color. The difference of streak-artefact appearances can be obviously recognized by viewing 3D images in Figure 8.

Irregular artefacts, which were caused by orthodontic wire and brackets, were observed at specific CT slices. Then we applied a very small ROI setting segmented from original images No.1 to No.4 of Figure 5, and Figure 9. The image in Figure 10 is an artefact-free image which is attached with the projection data (sinogram). It is the adjacent image of the far left one in Figure 9. As explained in the methodology section, the OS-EM successive iterative

restoration algorithm was applied on segmented images. Resultant images are shown in Figure 11 and they are corresponding to the order of Figure 9. Because of the decreasing calculation loading, the processing duration time reduced to 10.4 seconds for reconstructing a single small-ROI-setting image while it was 84 sec for a single original-sized CT slice. In the original ROI images, streak artefacts seriously damaged the image quality. And on the resultant images in Figure 11, tooth shape reverted to original state clearly and streak artefacts were also reduced effectively for both teeth and soft tissues.

As result of the calculation acceleration, the execution time was substantially reduced compared to that when not using GPGPU. The computational loading comparison is given in Table 2.

Discussion

In previous studies, successive iterative ML-EM algorithm and OS-EM algorithm were proved to be effective in reducing streak artefacts on dental and maxillofacial multi-detector row CT (MDCT) images.[22-24] It was decided to select the successive iterative OS-EM algorithm in this study as it is time-saving compared to the ML-EM algorithm. Another key point is that the image can be reconstructed to approximate to the targeted image using less iteration times.[24] The successive iterative correction can present a good result in streak artefact reduction and anatomical structure recovery because adjacent CT slices often depict

very similar anatomical structures nearby thin-thickness slices.

Very small ROI segmentation was employed in this study. There are two advantages of the small ROI image segmentation. On one hand, during image reconstruction, influences from other tissue structures were removed. On the other hand, the processing time for reconstructing each image was significantly shortened. By using the small ROI segmentation, the streak artefact reduction and anatomic structure recovery were realized satisfactorily.

We introduced CUDA programming on the GPGPU machine for improving performance. Since only the unrelated data can be divided for use of CUDA program, it was decided to split the projection acquisition procedure to multi threads, and this proved to be a time-consuming process. Applying thread splitting to alternative steps could further shorten the execution time, and will likely be one of our future investigations.

In conclusion, the statistical reconstruction method was applied for the streak artefact reduction on preoperative and postoperative evaluation in the dento-alveolar region. Two alternative algorithms were effective. Both software and hardware tools, such as the OS-EM, the small ROI and the GPGPU realized faster calculation and further improved the performance compared to the results of our previous studies.

References

1. Fleischmann D, Boas FE. Computed tomography—old ideas and new technology. Eur

Radiol 2011; 21:510-517.

2. Pan X, Sidky EY, Vannier M. Why do commercial CT scanners still employ traditional, filtered back-projection for image reconstruction? Inverse Probl 2009; 25; 1230009.
3. Desai GS, Thabet A, Elias AYA, Sahani DV. Comparative assessment of three image reconstruction techniques for image quality and radiation dose in patients undergoing abdominopelvic multidetector CT examinations. Br J Radiol 2013; 86: 20120161.
4. Gutman F, Gardin I, Delahaye N, Rakotonirina H, Hitzel A, Manrique A, et al. Optimisation of the OS-EM algorithm and comparison with FBP for image reconstruction on a dual-head camera: a phantom and a clinical 18F-FDG study. Eur J Nucl Med Mol Imaging 2003; 30: 1510-1519.
5. Hwang D, Zeng GL. Convergence study of an accelerated ML-EM algorithm using bigger step size. Phys Med Biol 2006; 51: 237-252.
6. Xu F, Xu W, Jones M, Keszthelyi B, Sedat J, Agard D, et al. On the efficiency of iterative ordered subset reconstruction algorithms for acceleration on GPUs. Comput Methods Programs Biomed 2010; 98: 261-270.
7. Silva AC, Lawder HJ, Hara A, Kujak J, Pavlicek W. Innovations in CT dose reduction strategy: application of the adaptive statistical iterative reconstruction algorithm. AJR Am J Roentgenol 2010; 194: 191-199. doi: 10.2214/AJR.09.2953.
8. Rashed EA, Kudo H. Statistical image reconstruction from limited projection data with

intensity priors. Phys Med Biol 2012; 57: 2039-2061.

9. Wang G, Frei T, Vannier MW. Fast iterative algorithm for metal artifact reduction in X-ray CT. Acad Radiol 2000; 7: 607-614.

10. Nahmias C, Lemmens C, Faul D, Carlson E, Long M, Blodgett T, et al. Does reducing CT artifacts from dental implants influence the PET interpretation in PET/CT studies of oral cancer and head and neck cancer? J Nucl Med 2008; 49: 1047-1052.

11. Shimamoto H, Kakimoto N, Fujino K, Hamada S, Shimosegawa E, Murakami S, et al. Metallic artifacts caused by dental metal prostheses on PET images: a PET/CT phantom study using different PET/CT scanners. Ann Nucl Med 2009; 23: 443-449.

12. Abdoli M, Ay MR, Ahmadian A, Dierckx RA, Zaidi H. Reduction of dental filling metallic artifacts in CT-based attenuation correction of PET data using weighted virtual sinograms optimizedby a genetic algorithm. Med Phys 2010;37:6166-6177.

13. Tohnak S, Mehnert AJ, Mahoney M, Crozier S. Dental CT metal artefact reduction based on sequential substitution. Dentomaxillofac Radiol 2011;40:184-190.

14. Gong XY, Meyer E, Yu XJ, Sun JH, Sheng LP, Huang KH, et al. Clinical evaluation of the normalized metal artefact reduction algorithm caused by dental fillings in CT. Dentomaxillofac Radiol 2013; 42: 20120105. doi: 10.1259/dmfr.20120105

15. Bal M, Spies L. Metal artifact reduction in CT using tissue-class modeling and adaptive prefiltering. Med Phys 2006;33:2852-2859.

16. Rinkel J, Dillon WP, Funk T, Gould R, Prevrhal S. Computed tomographic metal artifact reduction for the detection and quantitation of small features near large metallic implants: a comparison of published methods. J Comput Assist Tomogr 2008;32:621-629.

17. Moon SG, Hong SH, Choi JY, Jun WS, Kang HG, Kim HS, et al. Metal artifact reduction by the alteration of technical factors in multidetector computed tomography: a 3-dimensional quantitative assessment. J Comput Assist Tomogr 2008;32:630-633.

18. Prell D, Kyriakou Y, Beister M, Kalender WA. A novel forward projection-based metal artifact reduction method for flat-detector computed tomography. Phys Med Biol 2009;54:6575-6591.

19. Veldkamp WJ, Joemai RM, van der Molen AJ, Geleijns J. Development and validation of segmentation and interpolation techniques in sinograms for metal artifact suppression in CT. Med Phys 2010;37:620-628.

20. Meyer E, Raupach R, Lell M, Schmidt B, Kachelriess M. Normalized metal artifact reduction (NMAR) in computed tomography. Med Phys. 2010; 37: 5482-5493.

21. Boas FE, Fleischmann D. Evaluation of two iterative techniques for reducing metal artifacts in computed tomography. Radiology 2011; 259: 894-902.

22. Kondo A, Hayakawa Y, Dong J, Honda A. Iterative correction applied to streak artifact reduction in an X-ray computed tomography image of the dento-alveolar region. Oral Radiology 2010; 26: 61-65. doi: 10.1007/s11282-010-0037-6

23. Dong J, Kondo A, Abe K, Hayakawa Y. Successive iterative restoration applied to streak artifact reduction in X-ray CT image of dento-alveolar region. Intl J of Comput Assist Radiol Surg 2011; 6:635-640. doi: 10.1007/s11548-010-0544-2

24. Dong J, Hayakawa Y, Kannenberg S, Kober C. Metal-induced streak artifact reduction using iterative reconstruction algorithms in X-ray CT image of the dento-alveolar region. Oral Surg Oral Med Oral Pathol Oral Radiol 2013; 115: e63-e73. doi:10.1016/j.oooo.2012.07.436

Table 1 Execution steps of maximum likelihood-expectation maximization algorithm

Execution steps	*Procedures*
Step 1	Select the top ("headmost") image. Usually this is an image containing streak artefact. Set this as the initial image
Step 2	Calculate the detecting probability
Step 3	Compute projection data of initial image. Then compare it with projection data of the intact image in matrix pixel sequence
Step 4	Reconstruct the assumed image according to the projection data ratio obtained in Step 3
Step 5	Normalize the reconstructed image and set as the new initial ("headmost") image.
Step 6	Repeat Step 3 to Step 5 until achieving the iteration time setting

Table 2 The computational loading comparison concerned with different algorithms and GPGPU runtime environment

Successive iterative restoration	*Execution parameters*	*Processing time*
ML-EM	50 times iteration	6 min 10 s
OS-EM	8 subsets / 10 times iteration	1 min 24 s
OS-EM on GPGPU	8 subsets / 10 times iteration	20 s

Figure legends

Figure 1. Example of computing a 256 x 256 matrix image's projection data. Each row in the projection data represents the detectability value of the detector for a designated angle. The projection data was acquired in 360 directions with 1 degree intervals, so the pixel matrix was 256 x 360.

Figure 2. Continuous six original (unprocessed) maxilla slices. They are aligned from Head to Foot, from No.1, the far left on the top row, to No.6, the far right on the bottom row. The slices were obtained before the jaw deformity treatment operation. No orthodontic device or titanium plate was present.

Figure 3. An artefact-free image with the projection data to its right. The artefact-free image is the adjacent image of the far left one on the top row of Figure 2.

Figure 4. Resultant images processed by successive iterative OS-EM algorithm presented in the same sequence as in Figure 2.

Figure 5. Continuous seven original (unprocessed) maxilla slices from Head to Foot. The image volume was obtained post-surgery. Orthodontic wire and brackets, bone screws or titanium plates can be observed on some specific CT slices.

Figure 6. An artefact-free image and its projection data. The artefact-free image is the adjacent image of the far left one on the top row of Figure 5.

Figure 7. Reconstructed images by successive iterative OS-EM algorithm. They correspond to the seven images in Figure 5.

Figure 8. Volume-rendered images of maxilla. The left image is reconstructed by merging 10 sequential MDCT slices from Figure 5. They are before streak artefact reduction. The middle one is reconstructed by merging 10 MDCT slices from Figure 7. They are following streak artefact reduction. Different colors for each reconstructed image are used to compare the 3D renderings before and after surgery (right image).

Figure 9. ROI images of sequential images No.1 to No.4 in Figure 5. Part of left mandible was segmented as a small ROI. These are original images without processing. The pixel matrix for the ROI images is 166 x 196.

Figure 10. An artefact-free small-ROI-setting image. This was segmented from the artefact-free image of Figure 6.

Figure 11. The reconstructed ROI images by successive iterative OS-EM algorithm, corresponding in order to the sequence of images in Figure 9.

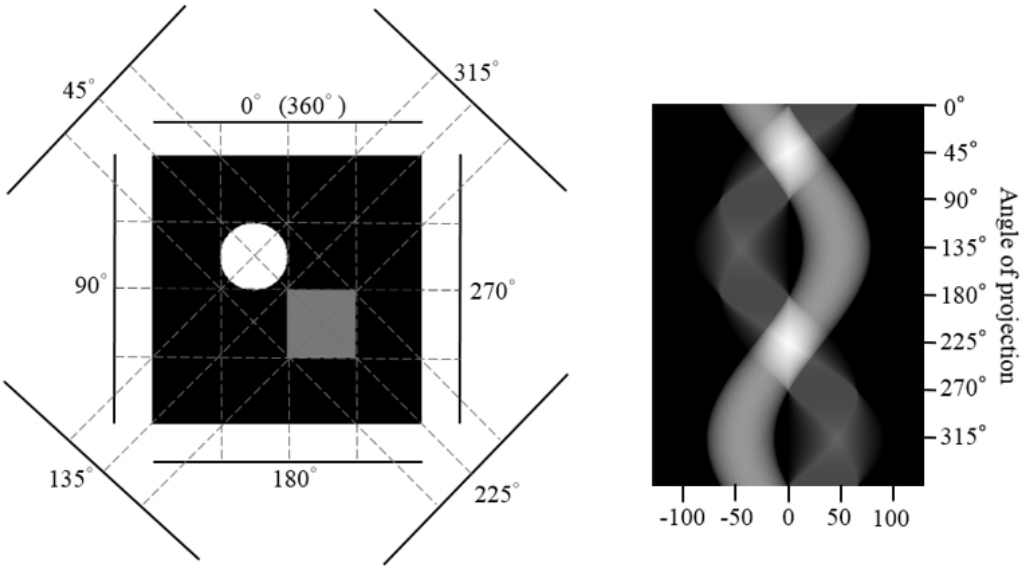

Original image data and its scanning
Matrix: 256 pixel x 256 pixel

Projection data (Sinogram)
Matrix: 256 pixel x 360 pixel

Figure 1.

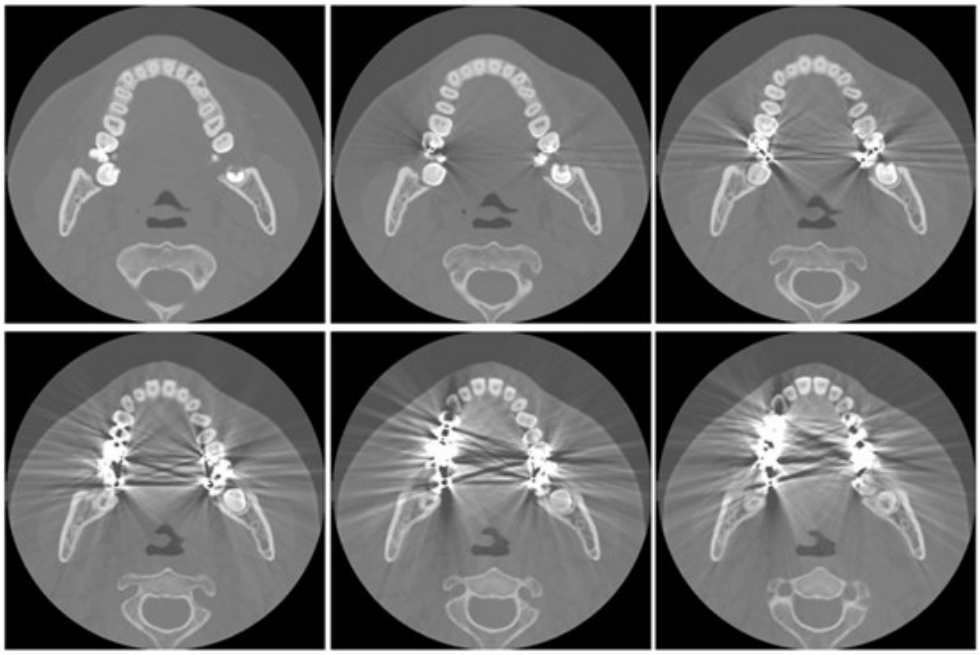

Figure 2.

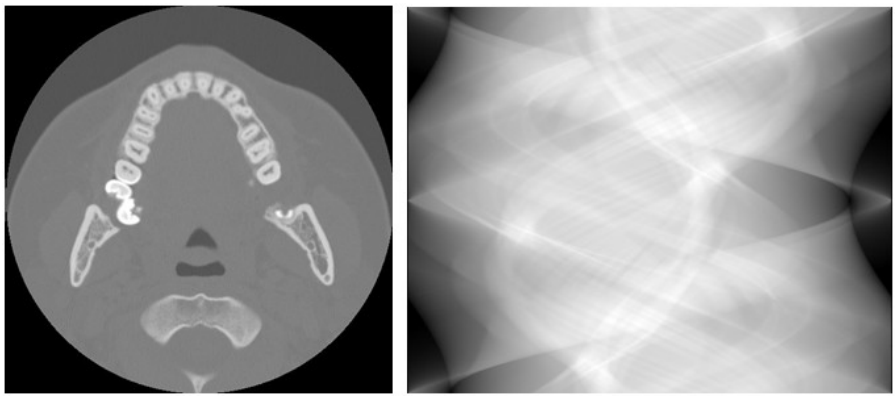

Figure 3.

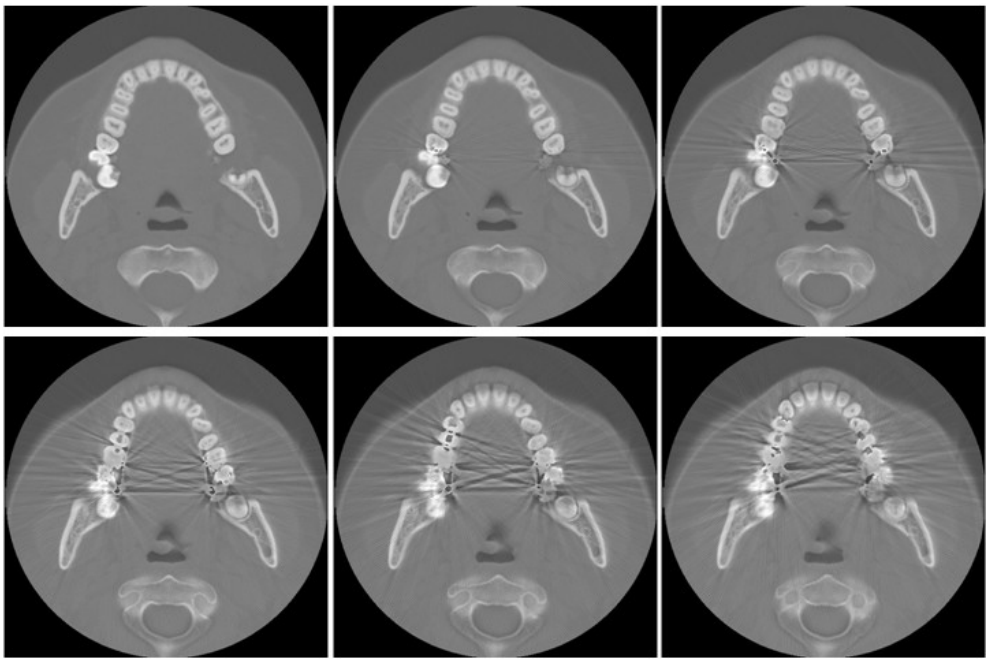

Figure 4.

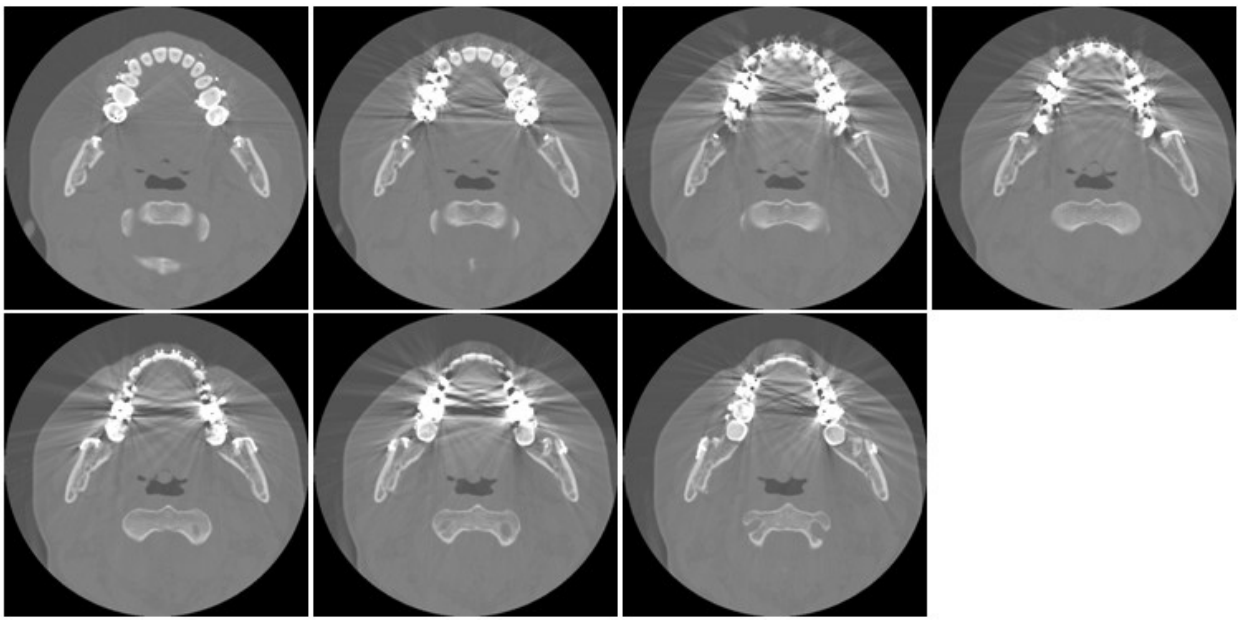

Figure 5.

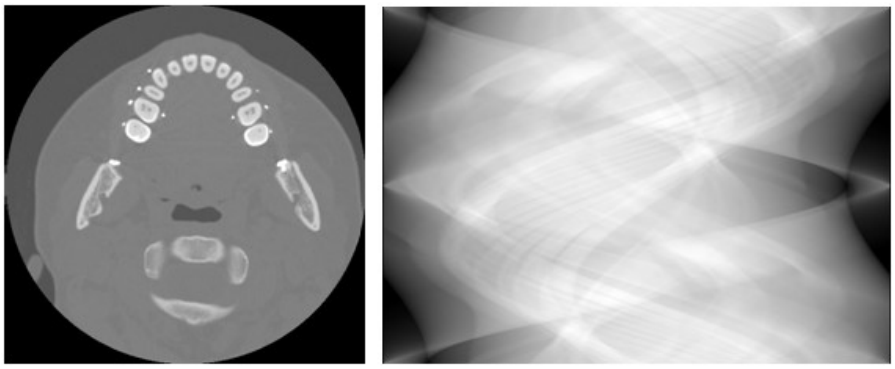

Figure 6.

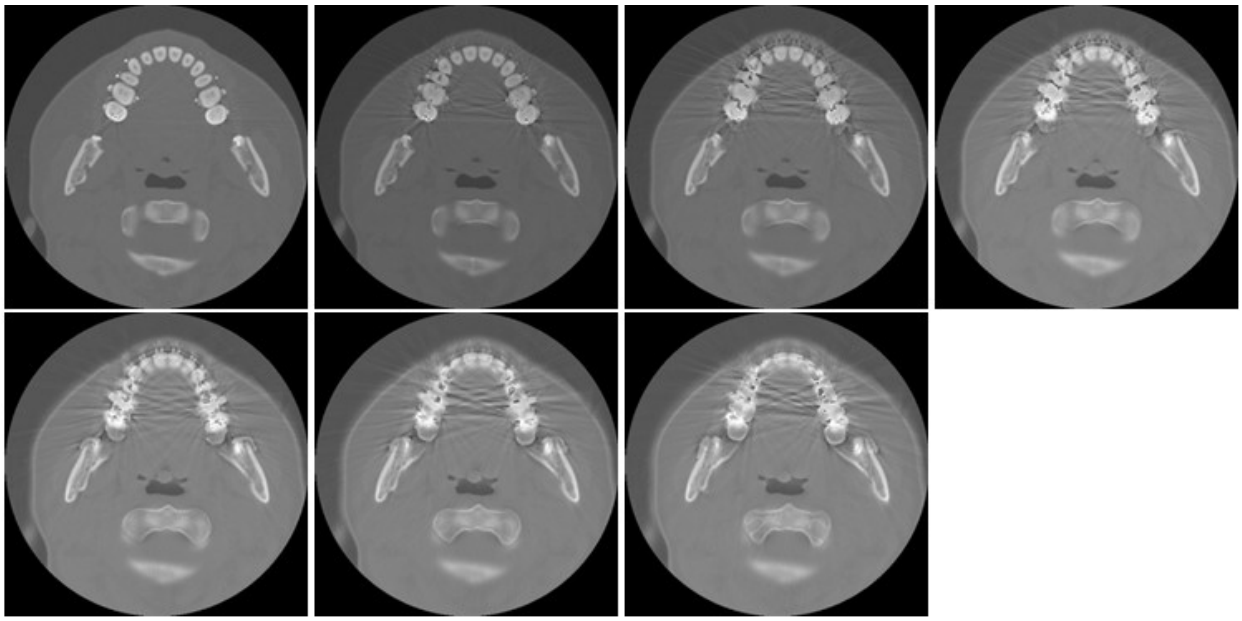

Figure 7.

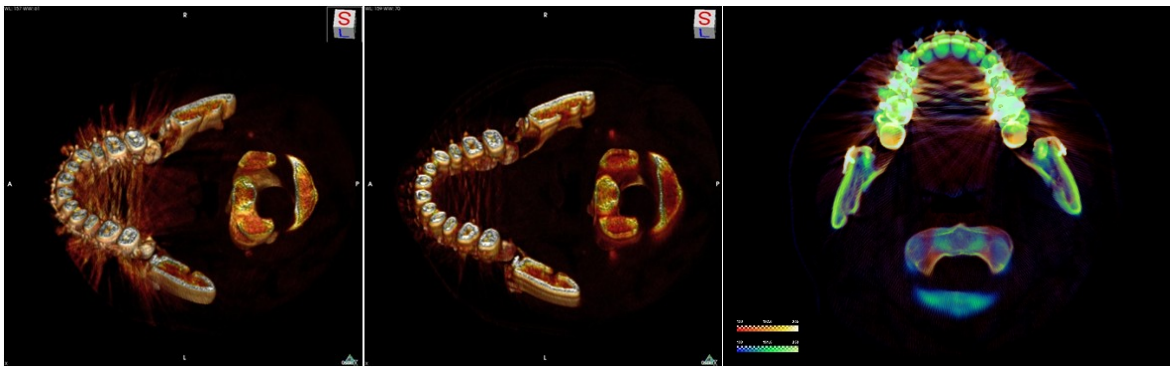

Figure 8.

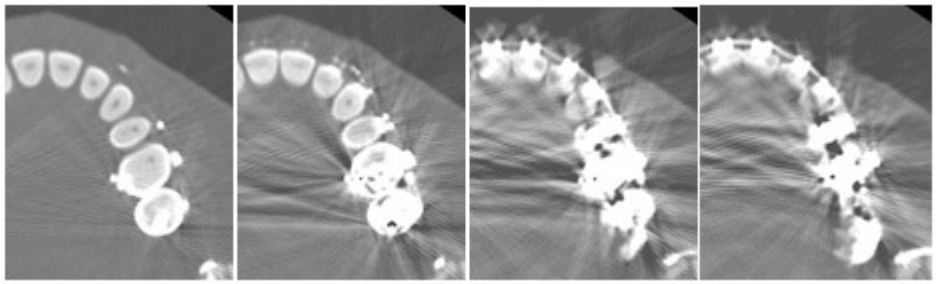

Figure 9.

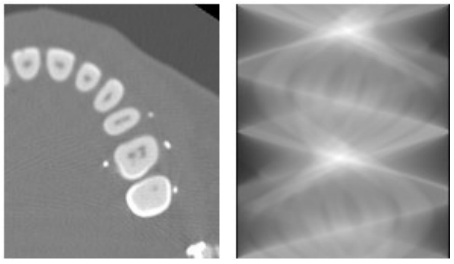

Figure 10.

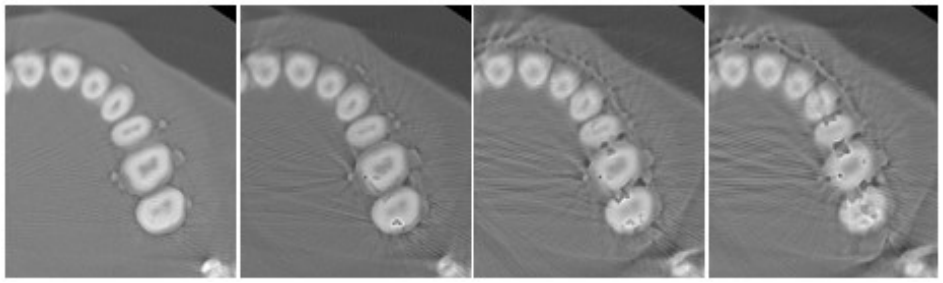

Figure 11.